Ceramics International 48 (2022) 25741–25746

Contents lists available at ScienceDirect

Ceramics International

journal homepage: www.elsevier.com/locate/ceramint

Characterization of temperature dependence of dielectric, elastic and piezoelectric properties of $BaTiO_3$ ceramics

Jing Hu [a,1], Heteng Fan [a,1], Songji Wu [a], Liguo Tang [a,c,*], Lei Qin [b,**], Wenyu Luo [c,d]

[a] Key Laboratory of Underwater Acoustic Communication and Marine Information Technology, Ministry of Education, College of Ocean and Earth Sciences, Xiamen University, Xiamen, 361010, China
[b] Beijing Key Laboratory for Sensors, Beijing Information Science & Technology University, Beijing, 100192, China
[c] State Key Laboratory of Acoustics, Institute of Acoustics, Chinese Academy of Sciences, Beijing, 100190, China
[d] University of Chinese Academy of Sciences, Beijing, 100049, China

ARTICLE INFO

Keywords:
$BaTiO_3$ ceramics
Characterization
Piezoelectric constants
Elastic constants
Resonant ultrasound spectroscopy

ABSTRACT

$BaTiO_3$ was the first lead-free piezoelectric material used to fabricate piezoelectric devices. However, there are no published results describing the temperature dependence of the full matrix material constants of $BaTiO_3$ ceramics, which is important for the fabrication of devices based on these materials. In this study, the temperature dependence of the elastic and piezoelectric properties of a $BaTiO_3$ ceramic sample from 20 °C to 80 °C was determined using resonant ultrasound spectroscopy. The clamped dielectric constants in the temperature range from 20 °C to 80 °C were measured using an impedance analyzer. The self-consistency of the results was guaranteed because only one sample was used in the entire characterization procedure. In addition, the reliability of the results was confirmed by comparing the directly measured free dielectric constants ε_{11}^{T} and ε_{33}^{T} and electric impedance spectra with those calculated using the complete sets of constants obtained in this study.

1. Introduction

Lead-zirconate-titanate–based piezoelectric ceramics (PZT) are dominant in electromechanical devices due to their excellent piezoelectric properties [1]. However, PbO is used in their production, which is hazardous to the environment. Thus, environmentally friendly lead-free piezoelectric materials have attracted considerable interest in recent years [2,3]. $BaTiO_3$ ceramics have been used for piezoelectric devices since the 1950s [1]. They can also be used as biomaterials due to their environmentally friendly properties. Liu et al. fabricated a piezoelectric porous $BaTiO_3$ scaffold to repair large segmental bone defects in sheep [4]. The piezoelectric properties of $BaTiO_3$ ceramics are inferior to those of PZT, limiting their wider application. Several efforts have been made to improve the electromechanical properties of $BaTiO_3$ ceramics. Acosta et al. presented a detailed review of the $BaTiO_3$-based piezoelectric materials [5]. Takahashi et al. successfully fabricated high-density $BaTiO_3$ ceramics with a high d_{33} of 350 pC/N using a pure, fine powder with a particle size of 100 nm [6]. Hoshina et al. investigated the effect of the grain size on piezoelectric properties of $BaTiO_3$ ceramics in detail [7]. Zhu et al. fabricated $BaTiO_3$ piezoelectric ceramics having high d_{33} values (>350 pC/N) from three kinds of $BaTiO_3$ powders synthesized by the hydrothermal method [8]. Zhao et al. designed $BaTiO_3$-based ceramics with improved temperature stability and high piezoelectricity [9,10].

The complete sets of dielectric, elastic and piezoelectric constants of $BaTiO_3$ ceramics must be characterized before the ceramics are used in electromechanical devices. Moreover, the temperature dependence of these constants also needs to be determined to evaluate the influence of temperature on their properties. However, compared with reports on the fabrication of $BaTiO_3$ ceramics, published results describing the characterization of their full matrix constants are scarce. Bechmann presented a complete set of the elastic, piezoelectric and dielectric constants of polarized $BaTiO_3$ ceramic [11]. Berlincourt and Jaffe measured the elastic and piezoelectric properties of $BaTiO_3$ single crystals using the electric resonant (ER) method [12]. Masakazu et al. determined the temperature dependence of the elastic compliance coefficients, s_{11}^{E} and

* Corresponding author. Key Laboratory of Underwater Acoustic Communication and Marine Information Technology, Ministry of Education, College of Ocean and Earth Sciences, Xiamen University, Xiamen, 361010, China.
** Corresponding author.
E-mail addresses: liguotang@xmu.edu.cn (L. Tang), qinlei@bistu.edu.cn (L. Qin).
[1] These authors contributed equally to this work.

https://doi.org/10.1016/j.ceramint.2022.05.245
Received 31 March 2022; Received in revised form 5 May 2022; Accepted 20 May 2022
Available online 24 May 2022

s_{33}^{E}, and the piezoelectric constants, d_{31} and d_{33}, using the ER method [13].

The combination of ultrasonic pulse-echo (UPE) and ER methods is often used to characterize the elastic and piezoelectric properties of piezoelectric materials [14]. However, multiple samples with significantly different geometries must be used during the characterization, leading to a self-consistency problem due to sample-to-sample variation. The problem worsens at higher temperatures [15]. To overcome this problem, the samples used in the characterization should be as few as possible. Resonant ultrasound spectroscopy (RUS) is an alternative method [16–22]. In RUS, the resonance frequencies of a solid sample of a specific size are determined by its material constants, and vice versa. This method was first proposed by Frazer and LeGraw to determine the elastic constants of a solid sphere [16]. Their RUS setup employed one transducer to excite the sample and receive its vibration. Soga and Anderson improved this setup by using two ultrasonic transducers to realize the transmitting and receiving functions [17]. The improved setup uses the transmitting and receiving ultrasonic transducers to fix the sample. It has become mainstream. Ohno first characterized the elastic properties of piezoelectric samples using RUS [18]. Compared with the UPE and ER methods, RUS has considerable advantages for the characterization of piezoelectric samples having a small size or strong anisotropy [19–22].

In this work, RUS was employed to characterize the temperature dependence of the elastic and piezoelectric properties of $BaTiO_3$ ceramics in the temperature range from 20 °C to 80 °C. The free and clamped dielectric properties in the same temperature range were determined from the low-frequency and high-frequency capacitances, respectively, which were directly measured from the same sample using an impedance analyzer. The self-consistency of the results was guaranteed because the complete sets of dielectric, elastic and piezoelectric constants were measured from the same sample.

2. Experimental methods

$BaTiO_3$ ceramics have a ∞mm point-group structure. The matrices of the elastic constant $\mathbf{c}^{E}$, piezoelectric constant $\mathbf{e}$, and dielectric constant $\boldsymbol{\varepsilon}^{S}$ can be formulated as

$$\mathbf{c}^{E}=\begin{bmatrix} c_{11}^{E} & c_{12}^{E} & c_{13}^{E} & 0 & 0 & 0 \\ c_{12}^{E} & c_{11}^{E} & c_{13}^{E} & 0 & 0 & 0 \\ c_{13}^{E} & c_{13}^{E} & c_{33}^{E} & 0 & 0 & 0 \\ 0 & 0 & 0 & c_{44}^{E} & 0 & 0 \\ 0 & 0 & 0 & 0 & c_{44}^{E} & 0 \\ 0 & 0 & 0 & 0 & 0 & \frac{c_{11}^{E}-c_{12}^{E}}{2} \end{bmatrix}, \tag{1}$$

$$\mathbf{e}=\begin{bmatrix} 0 & 0 & 0 & 0 & e_{15} & 0 \\ 0 & 0 & 0 & e_{15} & 0 & 0 \\ e_{31} & e_{31} & e_{33} & 0 & 0 & 0 \end{bmatrix}, \tag{2}$$

and

$$\boldsymbol{\varepsilon}^{S}=\begin{bmatrix} \varepsilon_{11}^{S} & 0 & 0 \\ 0 & \varepsilon_{11}^{S} & 0 \\ 0 & 0 & \varepsilon_{33}^{S} \end{bmatrix}, \tag{3}$$

respectively.

A $BaTiO_3$ sample was provided by Yu Hai Electric Ceramics Co., Ltd., China. Its geometrical parameters after grinding were 5.556 mm × 4.527 mm × 5.486 mm. The sample density was 5623 kg/m^3. According to the IEEE Standard on Piezoelectricity [23], the measurement of free dielectric constants is suggested to be made at a frequency substantially lower than the lowest resonance frequency of the crystal sample, while that of clamped dielectric constants is made at frequencies that are high compared to the principal natural frequencies of the sample but well below any ionic resonances, and sufficiently removed from high overtone resonance frequencies. In this study, the low-frequency capacitance at 5 kHz and high-frequency capacitance at 30 MHz in the temperature range from 20 °C to 80 °C were measured using an HP 4194 and HP 4195 impedance analyzer, respectively. An HP 16034E test fixture was connected to the HP 4194 impedance analyzer. An HP 16194A test fixture was connected to the HP 4195 impedance analyzer. The sample and the fixture were put into a KINGJO LK-80T temperature chamber during the measurement. The free and clamped dielectric constants were calculated from the capacitances measured at 5 kHz and 30 MHz, respectively. The RUS method is seldom used to determine the dielectric constants due to the following two reasons. First, the resonance frequencies of piezoelectric samples are insensitive to dielectric constants [24,25]. Therefore, the dielectric constants are difficult to precisely determine using RUS. Second, the greater the number of constants to be determined, the more difficult the RUS procedure is. Moreover, the dielectric constants can be precisely measured using the impedance analyzer. Therefore, it is not necessary to determine them using RUS.

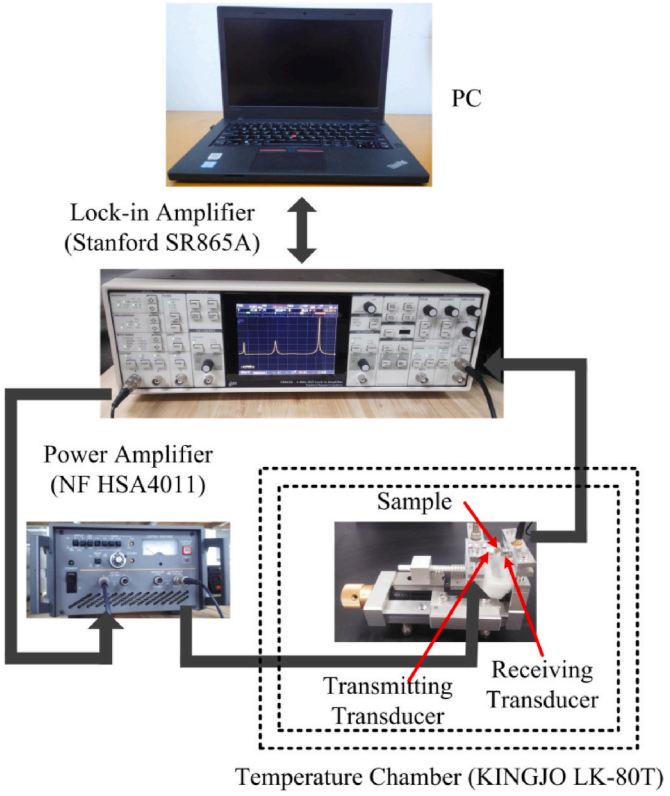

Fig. 1. RUS experimental setup.

Fig. 1 shows the RUS experimental setup, which includes a personal computer, a lock-in amplifier (Stanford SR865A), a power amplifier (NF HSA4011), a temperature chamber (KINGJO LK-80T), transmitting and receiving transducers, and the transducer fixer. Its workflow is given in Ref. [24]. The rectangular parallelepiped $BaTiO_3$ ceramic sample was fixed between the transmitting and receiving transducers and placed in a temperature chamber (KINGJO LK-80T). A thermocouple connected to a thermometer (Fluke 51-II) was used to measure the temperature of the $BaTiO_3$ sample inside the chamber. The resonant ultrasound spectra of the sample were measured in the temperature range from 20 °C to 80 °C at intervals of 5 °C.

Table 1
Free and clamped dielectric constants of $BaTiO_3$ ceramic sample at different temperatures.

T (°C)	$\varepsilon_{11}^T/\varepsilon_0$	$\varepsilon_{33}^T/\varepsilon_0$	$\varepsilon_{11}^S/\varepsilon_0$	$\varepsilon_{33}^S/\varepsilon_0$
20	1116	1305.	887	991
25	1114	1286	887	989
30	1113	1265	887	976
35	1118	1233	896	967
40	1135	1225	906	960
45	1152	1220	920	959
50	1177	1220	940	964
55	1213	1230	973	974
60	1247	1247	1002	991
65	1287	1272	1043	1015
70	1340	1309	1092	1037
75	1419	1333	1133	1082
80	1511	1347	1194	1131

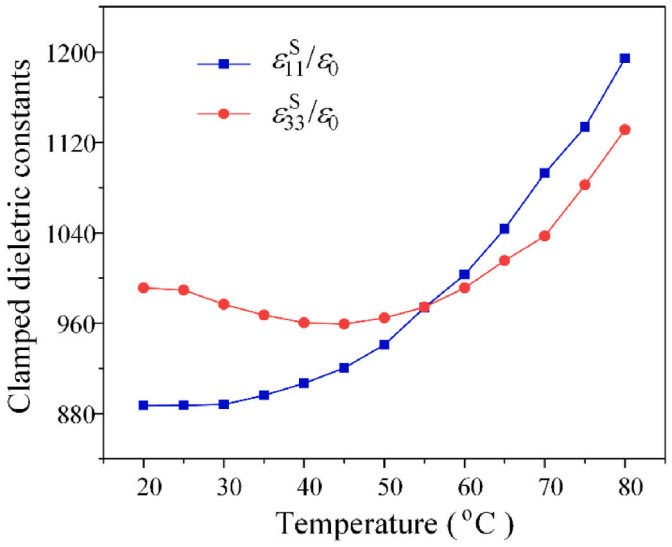

Fig. 2. Measured temperature dependence of clamped dielectric constants.

3. Results and discussion

3.1. Dielectric constants

Table 1 shows the free and clamped dielectric constants of the $BaTiO_3$ ceramic sample from 20 °C to 80 °C at intervals of 5 °C. Fig. 2 shows the temperature dependence of the clamped dielectric constants ε_{11}^S and ε_{33}^S. ε_{11}^S increases with an increase in temperature from 20 °C to 80 °C. ε_{33}^S decreases slowly with an increase in temperature from 20 °C to 45 °C, then increases with an increase in temperature from 50 °C to 80 °C.

3.2. Resonant ultrasound spectra

Fig. 3 shows the resonant ultrasound spectra from 20 °C to 80 °C at intervals of 10 °C. The resonance frequencies, for example, modes 2 and 9, increase with an increase in temperature from 20 °C to 60 °C; however, they are insensitive to temperature changes between 60 °C and 80 °C, as shown in Fig. 3. Fig. 4 shows the resonance frequencies as functions of temperature corresponding to modes 9–13.

Each peak in the resonant ultrasound spectra corresponds to a resonance mode. Identifying a sufficient number of resonance frequencies is one of the key steps in RUS. Mode omission and mode overlap cannot be avoided during the RUS measurement, which is a significant obstacle to mode identification. The mode identification process is summarized in Ref. [21]. Figs. 3 and 4 show that resonance frequencies vary slowly with temperature change. Thus, after the mode identification at the temperature T was successfully conducted, it could

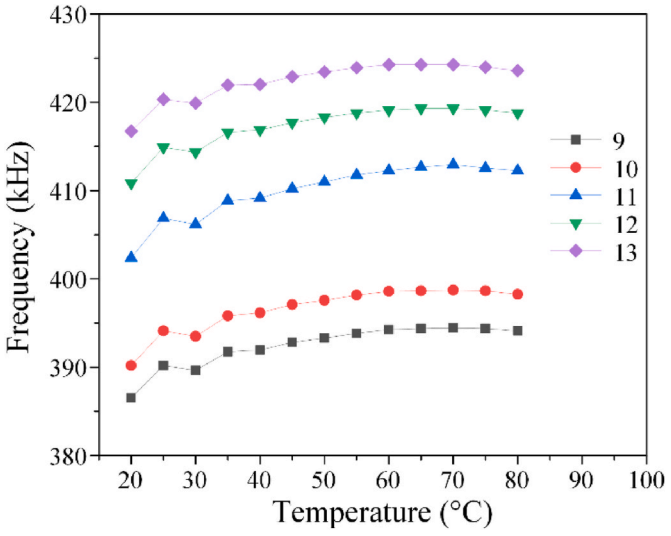

Fig. 4. Resonance frequencies as functions of temperature corresponding to modes 9–13.

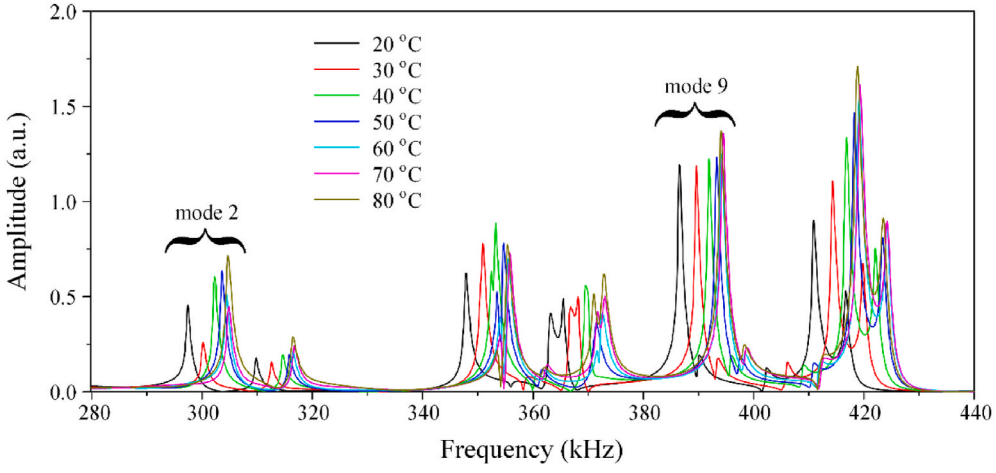

Fig. 3. Resonant ultrasound spectra from 280 kHz to 440 kHz at different temperatures.

Table 2
Resonance frequencies measured and those calculated from characterization results of barium titanate ceramics sample at 80 °C.

mode	f_{meas} (kHz)	f_{cal} (kHz)	Diff (%)[a]	mode	f_{meas} (kHz)	f_{cal} (kHz)	Diff (%)
1	231.08	230.23	0.37	41	694.84	695.62	0.11
2	304.75	303.75	0.33	42	700.46	701.63	0.17
3	316.39	316.55	0.05	43	711.5	712.81	0.18
4	353.5	354.06	0.16	44	719.96	719.93	0.004
5	355.39	355.69	0.08	45	720.98	720.8	0.02
6	361.96	361.97	0.002	46	–	–	–
7	370.96	371.04	0.02	47	736.14	735.95	0.03
8	372.86	373.01	0.04	48	748.33	748.14	0.03
9	394.12	394.08	0.01	49	753.67	753.58	0.01
10	398.25	398.73	0.12	50	766.6	768.87	0.3
11	412.26	412.63	0.09	51	777.97	779.03	0.14
12	418.76	418.12	0.15	52	–	–	–
13	423.57	423.67	0.02	53	–	–	–
14	–	–	–	54	–	–	–
15	469.74	470.15	0.09	55	806.13	803.27	0.36
16	487.49	487.64	0.03	56	–	–	–
17	491.21	492.29	0.22	57	–	–	–
18	496.22	495.53	0.14	58	820.68	820.73	0.01
19	503.87	503.33	0.11	59	827.12	823.18	0.48
20	507.19	506.47	0.14	60	–	–	–
21	524.73	523.9	0.16	61	834.36	835.83	0.18
22	527.17	526.55	0.12	62	837.88	839.86	0.24
23	530.22	529.74	0.09	63	842.21	843.71	0.18
24	–	–	–	64	843.90	843.92	0.002
25	536.11	535.2	0.17	65	–	–	–
26	563.26	563.43	0.03	66	854.93	856.09	0.13
27	572.07	572.58	0.09	67	856.29	857.35	0.12
28	586.02	586.87	0.15	68	–	–	–
29	589.40	590.60	0.20	69	866.64	866.47	0.02
30	606.87	607.95	0.18	70	869.28	867.72	0.18
31	609.18	610.34	0.19	71	–	–	–
32	627.6	627.93	0.05	72	874.5	873.61	0.10
33	–	–	–	73	881.33	883.77	0.28
34	648.72	648.41	0.05	74	883.50	884.65	0.13
35	–	–	–	75	888.10	889.81	0.19
36	–	–	–	76	898.25	898.39	0.01
37	662.06	662.88	0.12	77	903.74	902.64	0.12
38	665.86	667.92	0.31	78	908.48	909.48	0.11
39	673.58	673.92	0.05	79	919.10	921.44	0.25
40	686.24	685.92	0.05	80	925.53	927.9	0.26

[a] $\text{diff} = \left|\frac{f_{meas} - f_{cal}}{(f_{meas} + f_{cal})/2}\right| \times 100$

Table 3
Inversion results of elastic constants c_{ij}^{E} (10^{10}N/m^2) and piezoelectric constants e_{ij} (C/m^2).

T (°C)	C_{11}^{E}	C_{12}^{E}	C_{13}^{E}	C_{33}^{E}	C_{44}^{E}	e_{15}	e_{31}	e_{33}
20	16.65	7.10	7.03	16.43	4.75	9.71	−4.39	13.91
25	16.83	7.08	6.99	16.56	4.84	9.56	−3.89	13.91
30	16.82	7.08	7.03	16.53	4.84	9.56	−4.15	14.21
35	16.89	7.03	6.94	16.57	4.89	9.60	−3.98	13.83
40	16.92	7.03	6.94	16.58	4.90	9.65	−3.76	14.21
45	16.96	7.01	6.91	16.62	4.92	9.88	−3.45	14.13
50	16.90	6.91	6.85	16.58	4.93	9.81	−3.83	14.16
55	16.94	6.90	6.86	16.63	4.95	9.99	−3.62	14.42
60	16.90	6.84	6.78	16.56	4.96	10.12	−3.77	14.34
65	16.83	6.74	6.72	16.50	4.96	10.34	−3.62	14.94
70	16.79	6.68	6.67	16.47	4.97	10.56	−3.56	15.14
75	16.87	6.77	6.65	16.38	4.97	10.72	−2.73	16.13
80	16.83	6.73	6.61	16.31	4.96	10.98	−2.53	16.71

be followed to the next temperature step $T + \Delta T$, where ΔT is the temperature interval. In this work, 70 resonance frequencies were identified and used in the inversion. Table 2 lists 65 identified resonance frequencies between 200 kHz and 930 kHz at 80 °C.

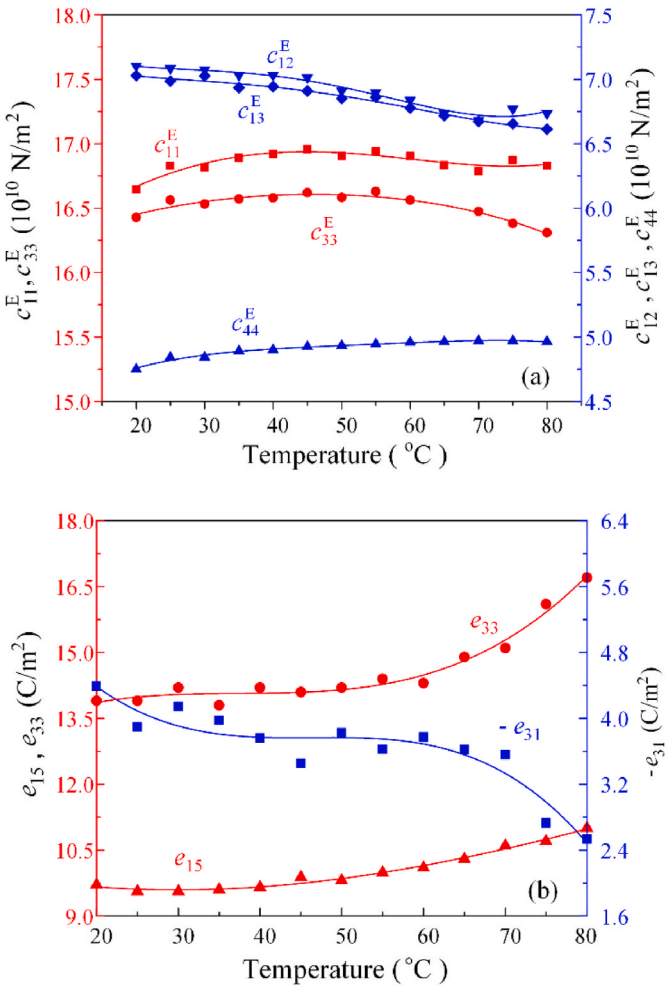

Fig. 5. Inversion results. (a) Elastic stiffness constants c_{11}^{E}, c_{12}^{E}, c_{13}^{E}, c_{33}^{E}, and c_{44}^{E}; (b) piezoelectric stress constants e_{15}, $-e_{31}$, and.e_{33}

3.3. Inversion

Inversion of the material constants from the resonance frequencies is performed to find a local minimizer of the following function:

$$F = \sum_{i=1}^{K} w_i \left[f_{cal}^{(i)} - f_{meas}^{(i)}\right]^2, \tag{4}$$

where $f_{meas}^{(i)}$ is the ith measured resonance frequency, $f_{cal}^{(i)}$ is the ith resonance frequency calculated using the material constants generated in the iteration process, and w_i is the weighting factor. This is a nonlinear least squares (NLS) problem. The Levenberg–Marquardt (LM) algorithm has been widely used to solve the NLS problem [26–28]. In this study, the LM algorithm was used as the inversion algorithm.

The elastic constants c_{ij}^{E} and piezoelectric constants e_{ij} of $BaTiO_3$ ceramics determined using RUS are shown in Table 3 and Fig. 5 f_{cal} in Table 2 corresponds to the resonance frequencies calculated using the elastic and piezoelectric constants at 80 °C, as shown in Table 3 f_{cal} can be obtained by solving the eigenvalue problem presented by Holland and Eer Nisse [29] using the variational method. The relative difference between the resonance frequencies calculated using the inversion results and those directly measured is given in Table 2. Most of the differences are less than 0.3%, indicating the reliability of the inversion.

Fig. 5(a) shows that c_{11}^{E} and c_{33}^{E} increase gradually with increasing temperature between 20 °C and 45 °C. c_{33}^{E} decreases slowly with increasing temperature between 55 °C and 80 °C. The maximal relative

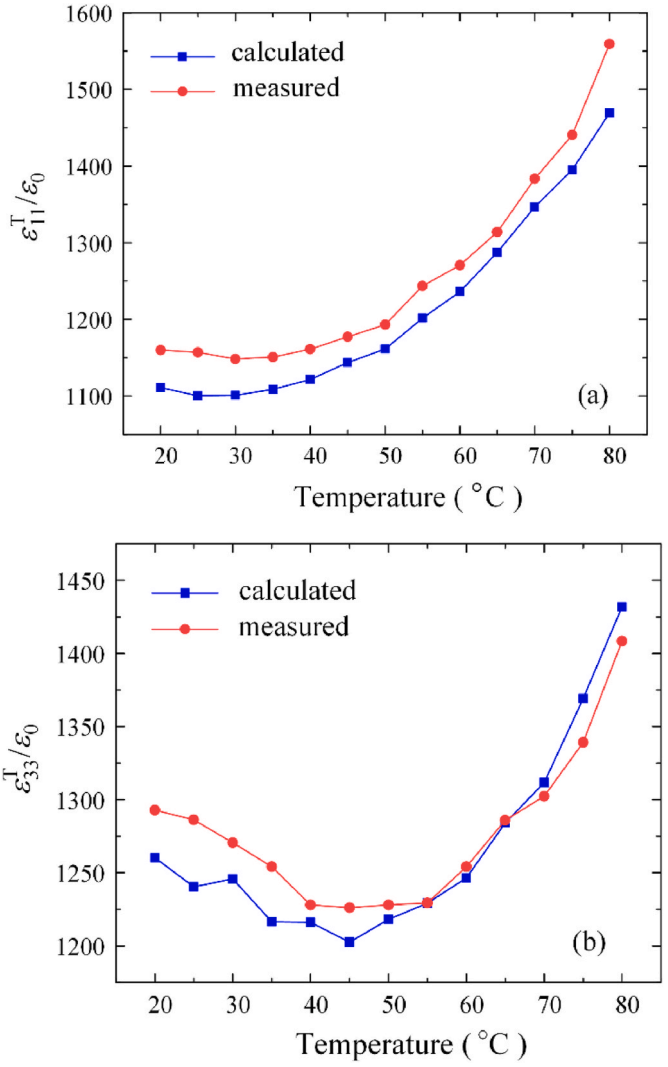

Fig. 6. Measured and calculated free dielectric constants. (a) ε_{11}^{T}; (b).ε_{33}^{T}

deviations of c_{11}^{E} and c_{33}^{E} between 20 °C and 80 °C are approximately 1.8% and 1.9%, respectively, indicating that they are insensitive to temperature in this range. The elastic constant c_{13}^{E} decreases with increasing temperature, whereas c_{44}^{E} increases with increasing temperature between 20 °C and 80 °C. c_{12}^{E}, c_{13}^{E}, and c_{44}^{E} are more sensitive to temperature than c_{11}^{E} and c_{33}^{E}. Fig. 5(b) shows that e_{15} and e_{33} increase with increasing temperature between 20 °C and 80 °C. The maximal relative deviations of e_{15} and e_{33} between 20 °C and 80 °C are 12.3% and 18.3%, respectively. They are more sensitive to temperature than the elastic constants.

The free dielectric constants ε_{11}^{T} and ε_{33}^{T} can be calculated using

$$\varepsilon_{11}^{T} = \varepsilon_{11}^{S} + e_{15} s_{55}^{E} e_{15} \tag{5}$$

and

$$\varepsilon_{33}^{T} = \varepsilon_{33}^{S} + 2e_{31}^{2}\left(s_{11}^{E} + s_{12}^{E}\right) + 4e_{31}e_{33}s_{13}^{E} + e_{33}^{2}s_{33}^{E}, \tag{6}$$

respectively, where s_{ij}^{E} is the elastic compliance constant at a constant electric field. The red line in Fig. 6 corresponds to the free dielectric constants measured using the impedance analyzer. The blue line in Fig. 6 corresponds to the free dielectric constants calculated using Eqs. (5) and (6). The relative difference $\left|(\varepsilon_{11(\mathrm{cal})}^{T} - \varepsilon_{11(\mathrm{meas})}^{T})/\varepsilon_{11(\mathrm{meas})}^{T}\right|$ is below 5.0% from 20 °C to 75 °C, and is 5.4% at 80 °C. The relative difference

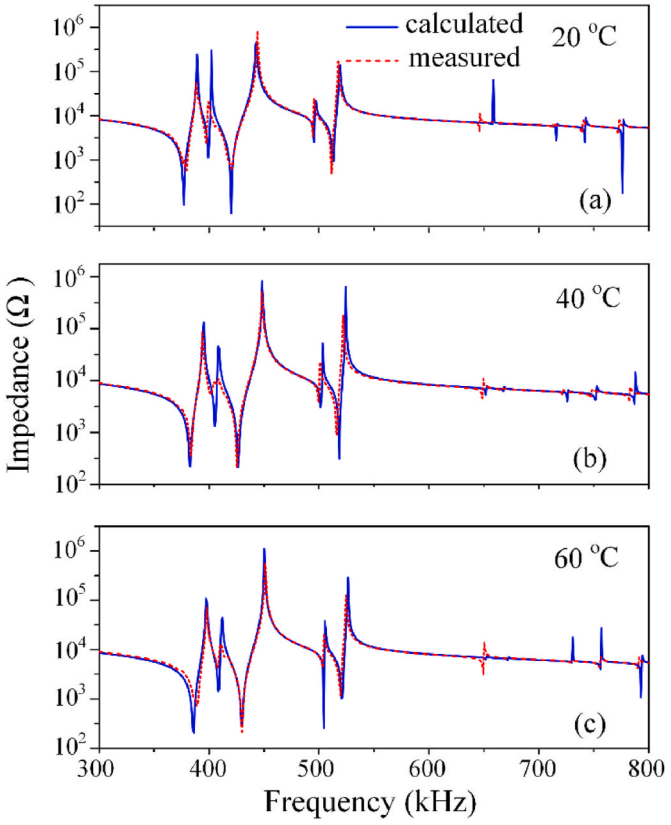

Fig. 7. Electrical impedance curves measured using the impedance analyzer (dashed red line) and calculated using FEM (solid blue line) from 300 to 800 kHz. (a) 20 °C; (b) 40 °C; (c) 60 °C.

$\left|(\varepsilon_{33(\mathrm{cal})}^{T} - \varepsilon_{33(\mathrm{meas})}^{T})/\varepsilon_{33(\mathrm{meas})}^{T}\right|$ is less than 3.6% in the full temperature range. $\varepsilon_{ii(\mathrm{meas})}^{T}$ and $\varepsilon_{ii(\mathrm{cal})}^{T}$ (i = 1 and 3) are the measured and calculated free dielectric constants, respectively.

The electrical impedance curve of the piezoelectric sample with a specific size is determined by its dielectric, elastic and piezoelectric constants. Thus, the reliability of the determined results can be checked by comparing the electrical impedance curve directly measured by the impedance analyzer with that calculated by the finite element method (FEM) using the determined material constants. Fig. 7(a)–(c) show the electrical impedance curves from 300 to 800 kHz at 20 °C, 40 °C, and 60 °C, respectively, where the dashed red lines were measured using the HP 4194 impedance analyzer, and the blue solid lines were computed using a commercial FEM software ABAQUS (Dassault Systèmes Simulia Corp., Providence, RI). The elastic and piezoelectric constants determined by RUS, as shown in Table 3, were used in the simulation. The clamped dielectric constants used in the simulation are shown in Table 1. Fig. 7 shows that the measured and simulated electrical impedance curves are in good agreement. Figs. 6 and 7 prove the reliability of the results determined in this study.

4. Conclusions

In summary, the temperature dependence of the complete set of dielectric, elastic and piezoelectric constants of $BaTiO_3$ ceramics was successfully characterized in the temperature range from 20 °C to 80 °C. The free and clamped dielectric constants were directly measured using an impedance analyzer. The elastic and piezoelectric constants were determined using the RUS method. Compared with the elastic constants, the piezoelectric constants were more sensitive to temperature. The self-consistency of the obtained results was guaranteed because only one sample was used in the characterization process. The reliability of the

results was confirmed by the good agreement between the directly measured and calculated free dielectric constants ε_{11}^{T} and ε_{33}^{T}, and between measured electrical impedance spectra and calculations using FEM.

Declaration of competing interest

The authors declare that they have no known competing financial interests or personal relationships that could have appeared to influence the work reported in this paper.

Acknowledgments

This work was supported by the National Natural Science Foundation of China (Grant Nos. U2006218 and 11674270), and State Key Laboratory of Acoustics, Chinese Academy of Science (Grant No. SKLA202108). The authors thank H.M. Zhu (Xiamen University) for her help in the preparation of the $BaTiO_3$ sample.

References

[1] B. Jaffe, W.R. Cook, H. Jaffe, Piezoelectric Ceramics, Academic Press, London, 1971.
[2] L.T. Yang, X. Kong, F. Li, H. Hao, Z.X. Cheng, H.X. Liu, J.F. Li, S.J. Zhang, Perovskite lead-free dielectrics for energy storage applications, Prog. Mater. Sci. 102 (2019) 72–108.
[3] J.G. Hao, W. Li, J.W. Zhai, H. Chen, Progress in high-strain perovskite piezoelectric ceramics, Mater. Sci. Eng. R. 135 (2019) 1–57.
[4] W.W. Liu, D. Yang, X.H. Wei, S. Guo, N. Wang, Z. Tang, Y.J. Lu, S.N. Shen, L. Shi, X. K. Li, Z.G. Guo, Fabrication of piezoelectric porous $BaTiO_3$ scaffold to repair large segmental bone defect in sheep, J. Biomater. Appl. 35 (2022) 544–552.
[5] M. Acosta M, N. Novak, V. Rojas, S. Patel, R. Vaish, J. Koruza1, G.A. Rossetti, J. Rödel, $BaTiO_3$-based piezoelectrics: fundamentals, current status, and perspectives, Appl. Phys. Rev. 4 (2017), 041305.
[6] H. Takahashi, Y. Numamoto, J. Tani, K. Matsuta, J. Qiu, S. Tsurekawa, Lead-free barium titanate ceramics with large piezoelectric constant fabricated by microwave sintering, Jpn. J. Appl. Phys. 45 (1) (2006). L30–L32.
[7] T. Hoshina, S. Hatta, H. Takeda, T. Tsurumi, Grain size effect on piezoelectric properties of $BaTiO_3$ ceramics, Jpn. J. Appl. Phys. 57 (2018), 0902BB.
[8] K.J. Zhu, J.H. Qiu, H.L. Ji, A. Totsuka, Fabrication of lead-free barium titanate piezoelectric ceramics from barium titanate powders with different particle sizes synthesized by hydrothermal method, Int. J. Appl. Electromagn. Mech. 31 (1) (2009) 9–16.
[9] C.L. Zhao, B. Wu, J.G. Wu, Composition-driven broad phase boundary for optimizing properties and stability in lead-free barium titanate ceramics, J. Am. Ceram. Soc. 102 (6) (2019) 3477–3487.
[10] C.L. Zhao, B. Wu, H.C. Thong, J.G. Wu, Improved temperature stability and high piezoelectricity in lead-free barium titanate-based ceramics, J. Eur. Ceram. Soc. 38 (16) (2018) 5411–5419.
[11] R. Bechmann, Elastic, piezoelectric, and dielectric constants of polarized barium titanate ceramics and some applications of the piezoelectric equations, J. Acoust. Soc. Am. 28 (3) (1956) 347–350.
[12] D. Berlincourt, H. Jaffe, Elastic and piezoelectric coefficients of single-crystal barium titanate, Phys. Rev. 111 (1) (1958) 143–148.
[13] M. Marutake, T. Ikeda, Anisotropy in polarized barium titanate ceramics, J. Phys. Soc. Jpn. 12 (3) (1957) 233–240.
[14] E.W. Sun, W.W. Cao, Relaxor-based ferroelectric single crystals: growth, domain engineering, characterization and applications, Prog. Mater. Sci. 65 (2014) 124–210.
[15] L.G. Tang, W.W. Cao, Temperature dependence of self-consistent full matrix material constants of lead zirconate titanate ceramics, Appl. Phys. Lett. 106 (5) (2015), 052902.
[16] D.B. Frazer, R.C. LeCraw, Novel method of measuring elastic and anelastic properties of solids, Rev. Sci. Instrum. 35 (9) (1964) 1113–1115.
[17] N. Soga, L. Anderson, Elastic properties of tektites measured by resonant sphere technique, J. Geophys. Res. 72 (6) (1967) 1733–1739.
[18] I. Ohno, Rectangular parallelepiped resonance method for piezoelectric crystals and elastic constants of alpha-quartz, Phys. Chem. Miner. 17 (5) (1990) 371–378.
[19] H. Ogi H, T. Ohmori, N. Nakamura, M. Hirao, Elastic, anelastic, and piezoelectric coefficients of alpha-quartz determined by resonance ultrasound spectroscopy, J. Appl. Phys. 100 (5) (2006), 053511.
[20] N. Nakamura, H. Ogi, M. Hirao, Elastic, anelastic, and piezoelectric coefficients of GaN, J. Appl. Phys. 111 (1) (2012), 013509.
[21] L.G. Tang, H. Tian, Y. Zhang, W.W. Cao, Temperature dependence of dielectric, elastic, and piezoelectric constants of [001]c poled Mn-doped $0.24Pb(In_{1/2}Nb_{1/2})O_3$ -$0.46Pb(Mg_{1/3}Nb_{2/3})O_3$-$0.30PbTiO_3$ single crystal, Appl. Phys. Lett. 108 (8) (2016), 082901.
[22] Y. Xiang, C.W. Chen, L.G. Tang, L. Qin, H.M. Zhu, W.W. Cao, Dielectric, elastic and piezoelectric properties of single domain $Pb(Zn_{1/3}Nb_{2/3})O_3$–6.5%$PbTiO_3$ single crystal with 3m symmetry measured using one sample, Scripta Mater. 194 (2021), 113634.
[23] IEEE Standard on Piezoelectricity, vol. 176, ANSI/IEEE Std, 1987.
[24] H. Li, Y.P. Ma, Z.J. Zhou, T.T. Yan, Y.X. Wu, L.G. Tang, S.X. Liu, X.Y. Wu, Characterizing full matrix constants of piezoelectric materials from one sample using resonant ultrasound spectroscopy, J. Mater. Sci. 54 (2019) 6786–6798.
[25] W. Wang, K. Zheng, S.S. Sun, L. Qin, L.G. Tang, Z.L. Li, Characterization of the full matrix constants of $Bi_4Ti_3O_{12}$ ceramics, Ceram. Int. 47 (2021) 23518–23527.
[26] K. Levenberg, A method for the solution of certain nonlinear problems in least squares, Q. Appl. Math. 2 (2) (1944) 164–168.
[27] D.W. Marquardt, An algorithm for least-squares estimation of nonlinear parameters, SIAM J. Appl. Math. 11 (1963) 431–441.
[28] J. Pujol, The solution of nonlinear inverse problems and the Levenberg-Marquardt method, Geophysics 72 (4) (2007) W1–W16.
[29] R. Holland, E.P. Eer Nisse, Variational evaluation of admittances of multielectroded three-dimensional piezoelectric structures, IEEE Trans. Sonics Ultrason. SU- 15 (1968) 119–132.